Increasing Contact-Ion Pairing as a Supercooled Water Anomaly. Estimation of the Fictive Temperature of Hyperquenched Glassy Water

Gerhard Fleissner, Andreas Hallbrucker, and Erwin Mayer*

Institut für Allgemeine, Anorganische und Theoretische Chemie, Universität Innsbruck, A-6020 Innsbruck, Austria

Received: April 7, 1998; In Final Form: May 5, 1998

In "dilute" aqueous D_2O solution of calcium nitrate, contact-ion pairing increases on cooling from 300 to 240 K, despite simultaneous increase of water's dielectric permittivity. This increase in contact-ion pairing was quantified by FT-IR spectroscopic evaluation of nitrate's ν_2 band region. The bound/free nitrate area ratios strongly increase on supercooling in a nonlinear way, in a similar manner as the anomalous molar volume of supercooled water does, which suggests that both anomalies have a common origin in the structural changes of supercooled water. By extrapolation of bound/free nitrate area ratios, we conclude that water and the solute become, on hyperquenching into the glassy state, immobilized between 230 and 200 K. This is important for analysis of the thermodynamic path liquid water takes on quenching into the glassy state, and it gives a low-temperature limit where conformational changes can occur in a biomolecule during quenching of its aqueous solution into the glassy state.

Introduction

The anomalies of water and dilute aqueous solution in their supercooled states at constant pressure, a topic of considerable interest and experimentally investigated in particular by Angell and co-workers (see refs 1−3 for reviews), had been attributed to structural changes toward a more open, fully hydrogen-bonded tetrahedral network in a comparatively small temperature region. These structural changes continue on "hyperquenching" liquid water on cooling at $\approx 10^6-10^7$ K s^{-1} into the glassy state.[4,5] The spatial correlation function of hyperquenched glassy water (HGW) obtained this way can be nicely modeled by a continuous random network of tetrahedrally connected H-bonded water molecules,[6,7] and this is consistent with structural changes occurring on supercooling liquid water.[8−10] During hyperquenching, the structure of liquid water becomes immobilized, or "frozen-in", at a temperature that must be much higher than that of its glass → liquid transition temperature (T_g) of 136 K determined by calorimetry on reheating at a rate of 30 K min^{-1}.[11,12] The temperature range where water becomes structurally immobilized on hyperquenching and its average fictive temperature (average T_f)[13,14] are of considerable theoretical and practical importance first for estimates of the thermodynamic path water takes on hyperquenching into the glassy state[15,16] and second because this temperature can be taken as a low-temperature limit for structural changes occurring in a solute on hyperquenching its dilute aqueous solution. Here we will discuss in particular conformational changes in a biomolecule when its aqueous solution is hyperquenched into the glassy state for further study by cryoelectron microscopy.[17−20]

We had previously observed by FT-IR or Raman spectroscopy for all "dilute" aqueous electrolyte solutions investigated so far that contact-ion pairing *increases* on hyperquenching into the glassy state.[21−26] This is unexpected because for aqueous electrolyte solutions studied on heating from ambient temperature, contact-ion pairing is known to increase with increasing temperature, mainly because of the parallel occurring decrease of water's dielectric permittivity.[27−31] Since in the glassy state both water and the dissolved electrolyte are immobilized in a nonequilibrium state, we had also started to investigate contact-ion pairing as a function of temperature in slow-cooled supercooled solution where the solution is in (metastable) equilibrium. For the two electrolytes thus investigated (i.e., sodium thiocyanate and calcium nitrate), qualitative evidence for anomalous increase in contact-ion pairing with decreasing temperature was observable by changes in peak heights in second- or fourth-derivative curves and in deconvoluted spectra.[21,22]

Here we report a quantitative study of anomalous increase in contact-ion pairing of "dilute" calcium nitrate solution on cooling from 300 to 240 K. This increase in contact-ion pairing was quantified by FT-IR spectroscopic evaluation of nitrate's ν_2 band region, and both the bound nitrate/free nitrate ratios and the apparent association constant strongly increase on supercooling in a nonlinear way, in a similar manner as the anomalous molar volume of supercooled water does.[1−3] This strongly supports our previous conjecture that increase in contact-ion pairing on supercooling a dilute aqueous electrolyte solution is an anomaly of supercooled water and that both the molar volume (i.e., density) anomaly and increasing contact-ion pairing might be caused by the same structural changes in supercooled water. By extrapolation of bound/free nitrate area ratios, we conclude that water and the solute become, on hyperquenching into the glassy state, immobilized between 230 and 200 K. These results are then discussed with respect to the anomalies of supercooled water[1−3] and recent molecular dynamics simulations of supercooled SPC/E water and its kinetic glass transition.[32−35]

By "dilute" we understand in this and the earlier studies[21−26] electrolyte concentrations which still show the anomalies of supercooled water,[1,2] although to a lesser extent. We studied 1.0 and 2.0 M $Ca(NO_3)_2$ solutions as examples for "dilute" solutions, both showing similar anomalous behavior. These are compared with a "concentrated", i.e., 5.0 M $Ca(NO_3)_2$ solution,

S1089-5647(98)01779-9 CCC: $15.00
Published on Web 07/18/1998

where normal behavior, i.e., decreasing contact-ion pairing on quenching into the glassy state, was observed.

Experimental Section

$Ca(NO_3)_2 \cdot 4H_2O$ (from Merck, p.a. quality) was dried over P_2O_5, and solutions were made with D_2O (99.7%). AgCl windows were used without spacer. The temperature was controlled by a calibrated thermocouple glued onto one of the AgCl windows. The 2.00 and 5.00 M $Ca(NO_3)_2$ D_2O solutions studied here correspond to 3.86 and 11.5 mol % salt, and the R values (R = water/salt mole ratio) are 24.9 and 7.70, respectively. A 25 wt % lanolin (Aldrich)/75% paraffine (Merck, Uvasol quality) mixture was used as emulsifier for the studies of supercooled solution in water/oil emulsion.[22,36,37] The influence of the emulsifier on spectral quality of solute bands is discussed in detail in refs 22 and 36. The mean water droplet diameter is $\sim 3\ \mu$m.[37] For discussion of the relationship between water droplet size and supercooling see ref 1.

The infrared spectra were recorded in transmission on Biorad's FTS 45 spectrometer at 2 cm^{-1} resolution (DTGS detector, UDR1; zero-filling factor 2; low-pass filter at 1.12 kHz; triangular apodization) by coadding between 250 and 1000 scans. Recording of the spectra was started at each temperature step after 5 min. Peak maxima are given in the figures to 0.1 cm^{-1} and were found to be reproducible to a few tenths of a wavenumber. Water vapor was subtracted from each spectrum. Data processing was performed with Spectra-Calc (Galactic). The sloping background was subtracted with a multipoint spline-function routine. The effects of baseline correction were controlled by comparing second-derivative curves of the original bands with those of the bands after subtraction of the sloping background. The effects of curve fitting were also controlled by comparison of second-derivative curves of the background-corrected composite bands with those of the sum of the curve-fitted component bands. This comparison of second (or fourth) derivatives allows reliable curve resolution of highly overlapping bands such as those of nitrate's ν_2 band region,[23,38] and development of this criterion for "goodness-of-fit" was essential for this study. All second-derivative curves are shown inverted.

The Raman spectrum of the 2.00 M $Ca(NO_3)_2$ D_2O solution was recorded at 295 K at ~ 4 cm^{-1} resolution (Raman spectrometer from DILOR, model LabRAM 1B). Curve resolution of the two bands centered at 715 and 735 cm^{-1} from "free" and bound nitrate gave a band area ratio of 2.03 to 1.00.

Results

An aquated nitrate ion is known to generate vibrational bands at $\approx$718 (ν_4, E′), $\approx$830 (ν_2, A″), $\approx$1049 (ν_1, A1′), and $\approx$1354 and 1410 cm^{-1} (ν_3, E′).[29] Lowering of the hypothetical D_{3h} symmetry is evident by splitting of ν_3 into two components and often by infrared activity of ν_1. Contact-ion pair formation is seen most clearly by development of a second band in the ν_4 band region at $\approx$740 cm^{-1}.[29] FT-IR spectroscopic study of contact-ion pairing via the ν_4 band region is now possible even for dilute nitrate D_2O solution by careful subtraction of the solvent bands.[23,26] However, this region cannot be used for emulsified samples because of intense bands of the emulsifier in this spectral region. FT-IR spectra of the ν_1 band region of dilute alkaline earth nitrate solutions in D_2O recorded in the glassy state can be separated into two components assignable to free and bound nitrate, but not those recorded at ambient temperature.[23] The degenerate ν_3 band region, although very intense and easy to separate from solvent bands, is too ambiguous for studies of contact-ion pairing.[23,29] Therefore, the ν_2 band region used in this FT-IR spectroscopic study for investigating contact-ion pairing is the only spectral region available, and it has the additional advantage to be a non-degenerate mode. This region can now be quantitatively studied for changes in contact-ion pairing after developing procedures for enhanced curve resolution of highly overlapping bands by comparison of second- or fourth-derivative curves.[25,26,38] We note that Raman spectroscopy, which has mainly been used for investigating contact-ion pairing in aqueous electrolyte solution, is not suitable for supercooled solution because of intense stray light from the emulsified samples. While Raman spectra of supercooled liquid water have been recorded at temperatures as low as 240 K even without emulsification and heterogeneous nucleation been avoided by using specially purified water,[39,40] this purification process is not possible for aqueous electrolyte solutions. Mossop's method to make water samples for supercooling close to the homogeneous nucleation limit is also not suitable for electrolyte solutions.[40]

$Ca(NO_3)_2$ as electrolyte was chosen because in our previous studies the ν_2 band region of the nitrate anion proved to be a sensitive indicator for ion pairing.[23,25,26] In addition, detailed Raman spectroscopic studies of ion pairing at ambient and elevated temperatures enable comparison with ion pairing in supercooled and glassy solution.[29,31,41−43] A 2.00 M solution was chosen as a compromise between sufficient signal-to-noise (S/N) ratio of the composite band in the ν_2 band region and low electrolyte concentration to probe the anomalous increase in contact-ion pairing of "dilute" supercooled solution. In emulsified 2.00 M $Ca(NO_3)_2$ solution in D_2O, the temperature range from 300 K down to 240 K could be investigated via FT-IR spectroscopy without formation of ice or crystalline hydrate. Formation of ice or crystalline hydrate on further cooling below 240 K is easily recognizable by sharp bands in the decoupled O−H stretching band region. Contact-ion pairing in supercooled and glassy 1.00 M solution was also studied,[44] giving similar results as the 2.00 M solution. These results are not shown here because the quality of the data is lower than those obtained with 2.00 M solution.

ν_2 Band Region of 2.00 M $Ca(NO_3)_2$ Solution. We first show in Figure 1 that emulsification and subtraction of a sloping background does not lead to artifacts. The spectrum in Figure 1a shows the ν_2 band region of an emulsified 2.00 M $Ca(NO_3)_2$ solution in D_2O recorded at 300 K and (a′) its inverted second derivative. Nitrate's ν_2 band region consists of two overlapping bands which are resolved in the second derivative (a′). Component bands centered at $\approx$830 and $\approx$826 cm^{-1} have been assigned to "free" (including solvent-separated and solvent-shared ion pairs) and "bound" (contact-ion paired) nitrate.[23,25,26,38,44] Both (a) and (a′) contain additional bands from the emulsifier. These emulsifier bands were subtracted in a first step by recording for each temperature a spectrum of the pure emulsifier phase and then by subtracting this spectrum from the spectrum of the $Ca(NO_3)_2/D_2O$ emulsion. This is shown in Figure 1b,b′ for the spectrum after subtraction of the emulsifier bands and for its second derivative. In a second step the sloping background was subtracted with a multispline function routine. Its spectrum, after subtraction of the background, is shown as (c) and its second derivative as (c′). Figure 1c′ further contains for comparison the second derivative of a 2.00 M $Ca(NO_3)_2$ solution in D_2O recorded also at 300 K which has not been emulsified (broken lines). The close correspondence between the second derivatives of the two spectra is taken as evidence that subtraction of the emulsifier bands does not lead to spectral artifacts. In the spectrum of the unemulsified solution the S/N

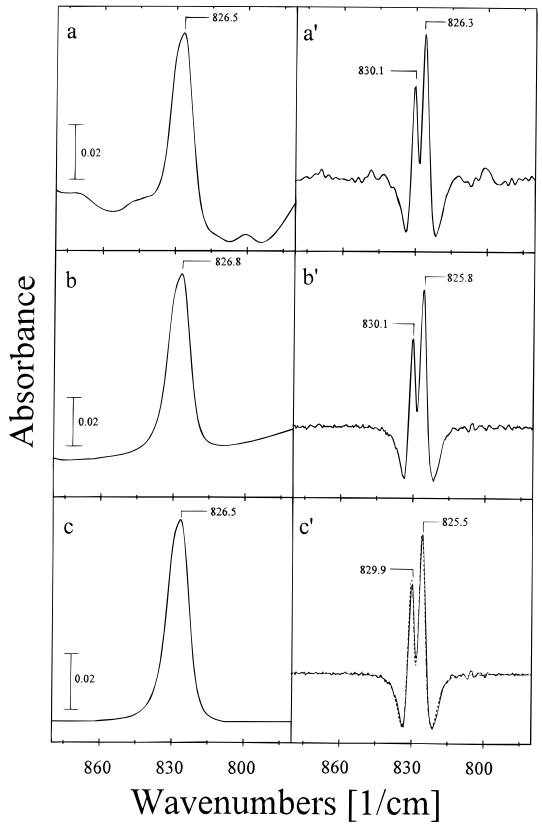

Figure 1. (a) Infrared spectrum of nitrate's ν_2 band region of an emulsified 2.00 M $Ca(NO_3)_2$ D_2O solution recorded at 300 K and its second derivative (a′); (b) the spectrum after subtraction of the emulsifier bands and its second derivative (b′); (c) the spectrum after subtraction of the sloping background with a multipoint spline function routine and the second derivative (c′, solid line); (c′) contains also the second derivative of a nonemulsified 2.00 M $Ca(NO_3)_2$ D_2O solution recorded at 300 K (broken line). Component bands at ∼830 and ∼826 cm^{-1} are from "free" and bound nitrate. The ordinate scale is given by the vertical bar. All second-derivative curves in this and the following figures are shown inverted.

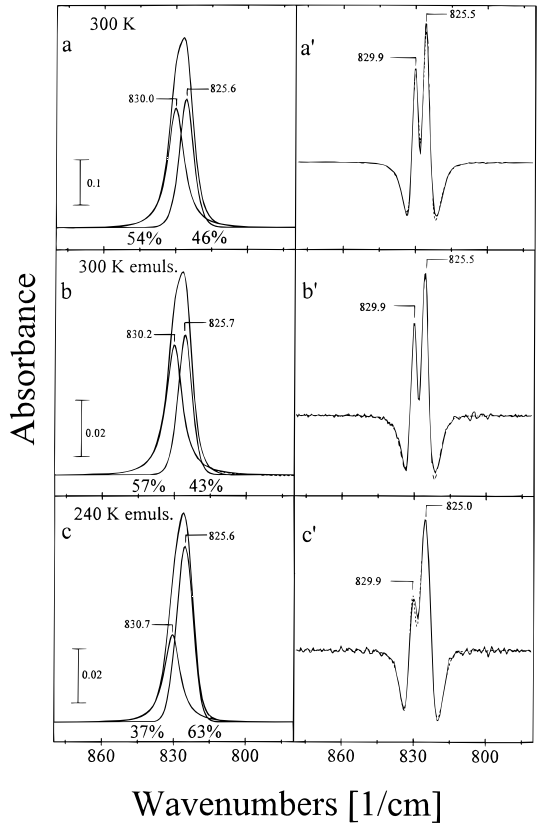

Figure 2. Comparison of the ν_2 band region of 2.00 M $Ca(NO_3)_2$ D_2O solution recorded at 300 K without emulsifier (a) and emulsified (b) and the curve-fitted component bands; (a′) and (b′) are the comparison of the second derivative of the experimental composite band (solid line) with that of the sum of the curve-fitted component bands (broken line); (c) shows the ν_2 band region of the emulsified 2.00 M $Ca(NO_3)_2$ D_2O solution recorded at 240 K and its curve-fitted component bands, and (c′) is the comparison of second derivatives as described for (a′) and (b′). Relative band areas of the two component bands are given in the figure. The spectra are shown after subtraction of emulsifier bands and of the sloping background. The ordinate scale is given by the vertical bar. Component bands at ∼830 and ∼826 cm^{-1} are from "free" and bound nitrate.

ratio is higher than in that of the emulsified solution, and consequently, the background-corrected second derivative of the former contains less noise than that of the latter.

In a third step reliable curve resolution of the composite band into the component bands due to "free" and bound nitrate was performed. Optimal correspondence between the second derivative of the composite band with that of the sum of the curve fitted component bands was used as criterion for "goodness-of-fit" (see Figure 1c). Details of this procedure are given in refs 26 and 38, and it provides a visual means for selecting the "best" fit. For this particular composite band we preferred the comparison of second derivatives to that of fourth derivatives used before[38] because the bands were resolved, and in emulsified samples the S/N ratio was too low for fourth derivatives. The "best" fit obtained by this comparison is shown in Figure 2b, including the curve-fitted component bands and their sum (broken line) and in Figure 2b′ the comparison of the second derivative of the experimental composite band (solid line) with that of the sum of the curve-fitted component bands (broken line). In Figure 2a we further show for comparison the background-corrected spectrum and the curve fit of unemulsified 2.00 M $Ca(NO_3)_2$, solution in D_2O recorded also at 300 K and in Figure 2a′ the comparison of second-derivative curves. The error in percentage is estimated as ±2, and therefore, band areas in Figure 2a,b are identical within experimental error.

In Figure 2c we further show the spectrum of a 2.00 M emulsified $Ca(NO_3)_2$ solution in D_2O recorded at 240 K, after subtraction of emulsifier bands and the sloping background, and the curve-fitted component bands. In Figure 2c′ the comparison of second-derivative curves is shown as criterion for the quality of the curve fit. The band area of "bound" nitrate shows pronounced increase upon cooling from 300 K (Figure 2b, 43%) down to 240 K (Figure 2c, 63%).

In Figure 3 the band area ratios I_B/I_F (i.e., bound/free nitrate), obtained by curve fitting, are plotted against temperature for 2.00 M $Ca(NO_3)_2$ solution in D_2O (open triangles, not emulsified) and in emulsion (solid triangles). Upside-down triangles are for I_B/I_F ratios obtained on cooling and upright triangles for those obtained on subsequent heating. The broken lines are shown to aid the eye. A slight increase of I_B/I_F with decreasing temperature is found in the 330−275 K temperature region but a marked nonlinear increase in the 275−240 K region. Differences of I_B/I_F ratios between emulsified and not emulsified solution may be due to some systematic error such as a slight change in concentration on emulsification. However, at low temperatures the changes of I_B/I_F ratios clearly exceed the experimental error, and therefore strongly increasing I_B/I_F ratio with decreasing temperature is significant. The "slight increase" of I_B/I_F ratio on cooling the unemulsified solution from 330 to

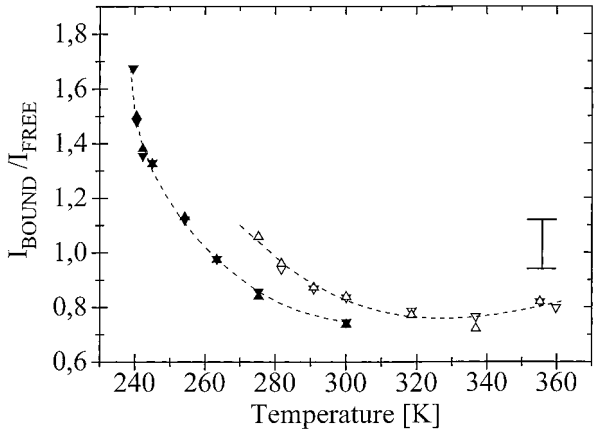

Figure 3. Plot of band area ratios I_{BOUND}/I_{FREE} versus temperature: open triangles, nonemulsified 2.00 M $Ca(NO_3)_2$ D_2O solution; full triangles, emulsified solution; upside-down triangles, ratios obtained from spectra recorded on cooling; upright triangles, those obtained on subsequent heating; the broken lines are drawn to aid the eye; the vertical bar indicates our error estimate.

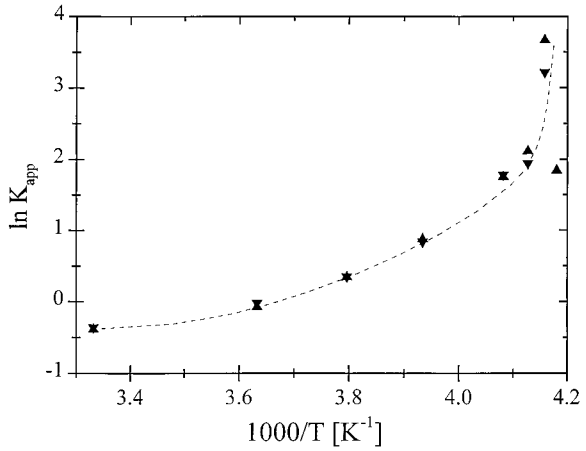

Figure 4. Plot of the logarithm of the apparent association constant, K_{app}, versus reciprocal temperature; the broken lines is drawn to aid the eye.

275 K may be within error. The error bar was calculated for the maximal error in band area evaluation by curve fitting (±2 in percentage). The difference between band area ratios obtained for the same temperature on cooling and subsequent heating is clearly smaller than the maximal error in band area evaluation, which is consistent with attainment of (metastable) equilibrium.

Apparent Association Constant, K_{app}. For the association reaction

$$Ca^{2+}{}_{aq} + NO_3^-{}_{aq} \leftrightarrow [Ca{\cdot}NO_3^+]_{aq} \quad (1)$$

the association constant is

$$K_{assoc} = [Ca{\cdot}NO_3^+]/[Ca^{2+}][NO_3^-] \quad (2)$$

For 2 M $Ca(NO_3)_2$ solution, evaluation of the ν_2 band region gave evidence for only two distinct bands assignable to "free" and bound nitrate. However, the solution must contain further species such as solvent-separated and solvent-shared ion pairs which are spectroscopically not separable from the band of "free" nitrate and are involved in further equilibra beyond that of eq 1. Therefore, the analysis of our data in terms of equilibrium (1) is an approximation, and only an apparent formation constant, K_{app}, can be calculated.[45]

The usual procedure for determining association constants is to obtain first the molar absorption coefficient for the band of the "free" ion, J_F, as a function of temperature by using an internal standard.[46] However, we do not know of an internal standard that can be used in supercooled solution without interfering. In glassy dilute aqueous solution even sodium perchlorate, which is often used as internal standard, shows evidence for perturbation of the perchlorate ion.[21] In the absence of a suitable internal standard, an estimation of K_{app} can nevertheless be obtained as follows. Careful Raman spectroscopic studies by Irish and co-workers have shown effectively equal molar absorption coefficients in the ν_4 band region of "free" and bound nitrate, i.e., $J_F = J_B$.[29,30,47] Therefore, by comparing integrated infrared band intensities of "free" and bound nitrate in the ν_2 band region with those of the ν_4 band region obtained by Raman spectroscopy for the same 2.00 M $Ca(NO_3)_2$ D_2O solution at 295 K, a J_F/J_B ratio of 0.65 was determined from the I_F/I_B ratio of the two infrared bands in the ν_2 band region of the emulsified solution. This J_F/J_B ratio allows to calculate the concentrations.

From the concentrations an apparent formation constant, K_{app} = [bound nitrate]/([Ca^{2+}][free nitrate]), is calculated. This assumes that the ratio of activity coefficients is 1, that J_B/J_F does not change with temperature, and that the "free" nitrate ion concentration contains contributions from solvent-separated and solvent-shared ion pairs. The logarithm of K_{app} is plotted against reciprocal temperature in Figure 4, and its increase with decreasing temperature is strongly nonlinear, in a similar manner as I_B/I_F.

Contact-Ion Pairing in "Concentrated" versus "Dilute" Solution. We next compare the temperature dependence of contact-ion pairing in "concentrated" $Ca(NO_3)_2$ solution, where the anomalies of supercooled water and aqueous solutions are expected to be absent,[1,2] with that of the "dilute" (2 M) solution shown above. A 5 M $Ca(NO_3)_2$ solution is used as "concentrated" solution, and it can be supercooled slowly into the glassy state without formation of ice or a crystalline hydrate. Therefore, emulsification is not necessary here, and it is possible to evaluate the ν_4 band region for changes in ion pairing. In Figure 5 we show that increase in contact-ion pairing on quenching into the glassy state is restricted to "dilute" solution and that the "concentrated" solution shows the opposite behavior. Here we compare curve fits of nitrate's ν_4 band region in 2 M $Ca(NO_3)_2$ solution in D_2O recorded 300 K (a) and after hyperquenching into the glassy state, at 78 K (c), with those of a 5.00 M $Ca(NO_3)_2$ solution recorded in D_2O solution at 295 K (b) and in the glassy state at 78 K obtained either by hyperquenching (d) or by slow cooling at a rate of ≈5 K min^{-1} (e). Component bands at ≈720 cm^{-1} are from "free" nitrate and at ≈740 cm^{-1} from bound nitrate.[29] Figure 5a,c (left) show the expected increase of bound nitrate on hyperquenching a 2 M solution into the glassy state from 59% at 295 K to 76% at 78 K, which is consistent with our previous reports.[21−24] For 5 M solution (right), however, the relative band area of bound nitrate decreases in going from 295 to 78 K from 86% (b) to 79% (d) and 80% (e). For 5 M glassy $Ca(NO_3)_2$ solution recorded at 78 K, the relative band areas of free and bound nitrate are identical within experimental error for the hyperquenched (d) and slow-cooled solution (e).

In the same manner, opposite temperature dependence of contact-ion pairing in "dilute" and "concentrated" $Ca(NO_3)_2$ D_2O solution is shown for the ($\nu_1 + \nu_4$) combination band region from 1770 to 1850 cm^{-1}.[23] Figure 6 (left) shows curve fits of

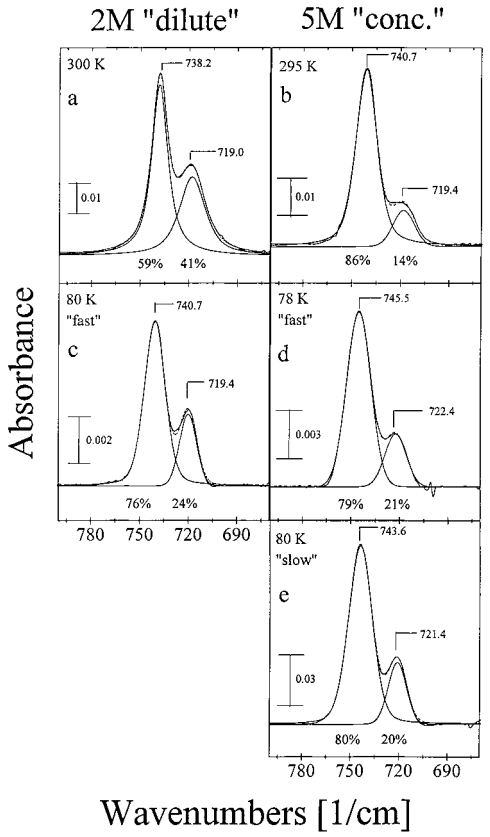

Figure 5. Comparison of the temperature dependence of contact-ion pairing in "dilute" 2.00 M $Ca(NO_3)_2$ D_2O solution with that in "concentrated" 5.00 M solution as seen in nitrate's ν_4 band region: (a) and (c) show spectra of 2 M solution recorded at 300 K (a) and at 80 K (c) after hyperquenching into the glassy state and their curve-fitted component bands; (b) and (d) show spectra of 5 M solution recorded at 295 K (b) and at 78 K (d) after hyperquenching into the glassy state and their curve-fitted component bands; (e) is the spectrum of a 5 M solution recorded at 80 K after slow cooling into the glassy state at $\approx$5 K min^{-1} and the curve-fitted component bands; broken lines are for the sum of the curve-fitted component bands, and vertical bars give the ordinate scales; the spectra are shown after subtraction of the solvent band. Component bands at $\sim$720 and $\sim$740 cm^{-1} are from "free" and bound nitrate. Note the increase in contact-ion pairing with decreasing temperature for 2 M solution and the opposite effect for 5 M solution.

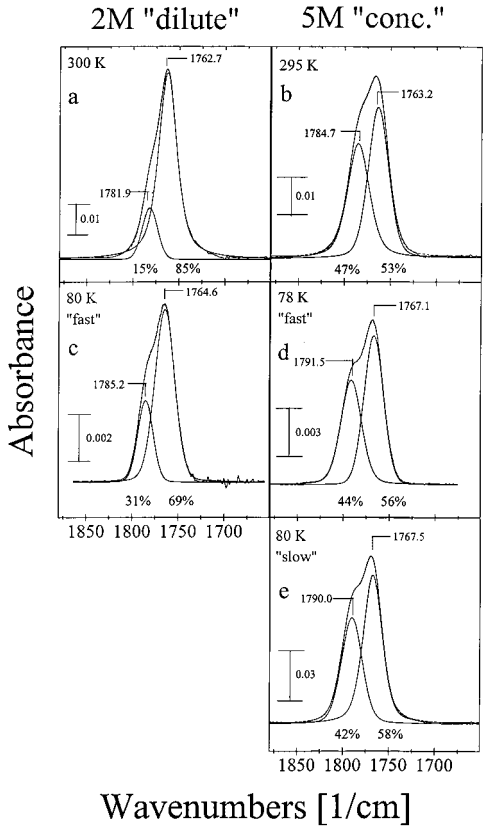

Figure 6. Comparison of the temperature dependence of contact-ion pairing in "dilute" 2.00 M $Ca(NO_3)_2$ D_2O solution with that in "concentrated" 5.00 M solution as seen in nitrate's combination band ($\nu_1 + \nu_4$) region: (a) and (c) show spectra of 2 M solution recorded at 300 K (a) and at 80 K (c) after hyperquenching into the glassy state and their curve-fitted component bands; (b) and (d) show spectra of 5 M solution recorded at 295 K (b) and at 78 K (d) after hyperquenching into the glassy state and their curve-fitted component bands; (e) is the spectrum of a 5 M solution recorded at 80 K after slow cooling into the glassy state at $\approx$5 K min^{-1} and the curve-fitted component bands; broken lines are for the sum of the curve-fitted component bands, and vertical bars give the ordinate scales; the spectra are shown after subtraction of the sloping background. Component bands at 1763−1768 and 1782−1792 cm^{-1} are from "free" and bound nitrate. Note the increase in contact-ion pairing with decreasing temperature for 2 M solution and the opposite effect for 5 M solution.

the 2 M solution recorded at 300 K (a) and after hyperquenching into the glassy state (c). The component band centered at higher frequency had been assigned to bound nitrate,[23,49] and its area increases from 15% (a) to 31% (c). For the "concentrated" (5 M) solution, however, the opposite temperature dependence is observed (Figure 6, right). The relative band area of bound nitrate decreases slightly in going from 295 K from 47% (b) to 44% and 42% at 80 K in hyperquenched (d) and slow-cooled (e) solution. This is consistent with the results for the ν_4 band region shown in Figure 5. We note that for 5 M $Ca(NO_3)_2$ solution a third component band had to be entered in the curve fit of the ν_2 band region, and because of that, no comparison is made with "dilute" 2 M solution.[26,38]

Discussion

Increasing contact-ion pairing has been observed as a general phenomenon for "dilute" aqueous electrolyte solution in going from ambient temperature to the glassy state by hyperquenching.[21−26] For thermodynamic reasons strongly increased contact-ion pairing cannot be due to liquid−liquid immiscibility and phase separation during hyperquenching into solute-rich and a water-rich phase, as pointed out in detail before.[23,50] Absence of phase separation on hyperquenching is also consistent with increasing contact-ion pairing in homogeneous supercooled (metastable) solution (Figures 3 and 4).

In the following we use the results obtained with 1 M (ref 44, not shown here) and 2 M solution as examples for "dilute" solution where the temperature of maximum density (TMD) and the anomalies of supercooled aqueous solution still exist[1,2,51] and those obtained with 5 M solution as example for "concentrated" solution where the density maximum has disappeared and anomalies of supercooled solution are absent.[1,2,51] This is an assumption because of experimental difficulties the concentration dependence of the TMD has not been determined for aqueous $Ca(NO_3)_2$ solution. Determination of TMD of an aqueous electrolyte solution requires deep supercooling for observing unambiguously the so-called "wash-out" concentration where the density maximum disappears.[1,51] For that special purification procedures are necessary in order to avoid heterogeneous nucleation for measurements in glass capillaries.[51] These procedures have been applied successfully to aqueous solutions of nonelectrolytes[1,51] but to our knowledge not to

electrolyte solutions. Our assumption is consistent with C_p versus temperature data for concentrated aqueous $Ca(NO_3)_2$ solutions (with $R = 2.86$, 4, 6, 8, and 12) obtained by differential scanning calorimetry on heating at 10 K min^{-1} reported by Angell and Tucker and their extrapolation to dilute solutions (see Figures 1 and 2 in ref 52).

Anomalous Contact-Ion Pairing in "Dilute" Supercooled Solution. The Fuoss−Kraus equation often used for describing ion pairing is[27,53]

$$K_A = \frac{4\pi N_0 a^3}{3000} \exp\left(\frac{|Z_i Z_j| e^2}{a\epsilon_0 kT}\right) \qquad (3)$$

where K_A is the association constant, a is the minimum distance between ions, z_i and z_j are the valence of ions i and j, e is the electron charge, T is the temperature in kelvin, and ϵ_0 is the static dielectric permittivity (or constant). At ambient and high temperatures, the degree of association depends mainly on the $\epsilon_0 T$ product. The $\epsilon_0 T$ product decreases with increasing T when the decrease in ϵ_0 outweighs the change in T. This decrease in ϵ_0 with increasing T is considered to be the main factor for increasing contact-ion pairing with increasing T.[27−31,54] Increasing contact-ion pairing with increasing T has been reported from Raman spectroscopic studies of $Ca(NO_3)_2$ dissolved in water from 296 to 723 K (see Figure 13 in ref 31) and in ammonia from 233 to 335 K (see Table I in ref 43).

The density maximum of "dilute" aqueous electrolyte solutions prevents meaningful extrapolation of the temperature dependence of contact-ion pair formation from data obtained at ambient and elevated temperatures into the supercooled and glassy state.[22,23] For two states of equal density above and below the TMD, very different properties and structures are to be expected; for example, for the same H_2O water density of $\approx$0.95 g cm^{-3}, the viscosity is $\gg 10^{14}$ P for glassy water at 77 K and $\approx 10^{-2}$ P for water at 384 K.[22] For H_2O water ϵ_0 increases on cooling from 305 to 257 K from 76 to 95; i.e., its $\epsilon_0 T$ product increases by $\approx$5% (calculated from the data in ref 55). According to eq 3 one would therefore expect a decrease in contact-ion pairing on supercooling whereas Figures 3 and 4 demonstrate clearly the opposite. We conclude that for "dilute" aqueous solutions the $\epsilon_0 T$ product and, more generally, the Fuoss−Kraus eq 3 cannot be used as indicator for ion association beyond the TMD because of water's density maximum and its structural changes on supercooling toward a more open network in a comparatively small temperature region.[1−3,8−10]

In "concentrated" aqueous solution, water's density maximum is "washed out", and the anomalies of supercooled water and of "dilute" aqueous solutions disappear.[1−3,51] This is consistent with our findings that in our "concentrated", 5 M, $Ca(NO_3)_2$ D_2O solution "normal" behavior occurs; i.e., a slight decrease in relative band area of bound nitrate in going from ambient to the supercooled and glassy state is observed (see Figures 5 and 6).

The plot of the logarithm of K_{app} against reciprocal temperature in Figure 4 shows pronounced nonlinear behavior. For linear relationship between the logarithm of an equilibrium constant against the reciprocal temperature for evaluation of the standard reaction enthalpy, $\Delta H°$, and entropy, $\Delta S°$, one assumption is that the difference between the heat capacities of products (bound nitrate) and reactants (free nitrate), ΔC_P, is negligible over the temperature range in question.[29] The pronounced deviation from linearity is an indication that this assumption is not valid for ion-pairing equilibria in supercooled "dilute" aqueous solution. From the positive slope of the plot in Figure 4 we conclude that the contact-ion pair formation in supercooled solution, below water's TMD, is an exothermic process. In contrast, a negative slope is usually obtained in ln K versus $1/T$ plots for formation of contact-ion pairs (or inner-sphere complexes) at ambient and elevated temperatures in aqueous solution above water's TMD and in nonaqueous solution. It follows that in the latter case contact-ion pairing is an endothermic process and ΔS is positive (see Table 1 in ref 29 and Table 2 in ref 56). Chingakule et al.[56] conclude from their studies of contact-ion pair formation in liquid ammonia that "the driving force in the ion association process derives from solvent−solute restructuring, and not the energy of interaction between the cation and anion". Our observation of an exothermic ΔH value for contact-ion pairing in supercooled "dilute" aqueous solution obviously requires a different interpretation.

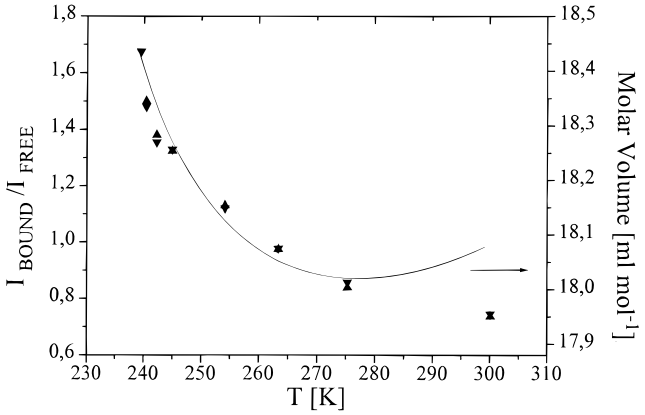

Figure 7. Comparison of the temperature dependence of I_{BOUND}/I_{FREE} area ratios with that of the molar volume of H_2O water (solid line). Density values of supercooled water are taken from Table 2 in ref 40.

In Figure 7 we compare the temperature dependence of I_B/I_F nitrate area ratios (data points) with that of the molar volume of H_2O water (solid line). Density values reported by Hare and Sorensen for supercooled water in glass capillaries with 0.3 mm inner diameter were used for calculating the molar volume (from Table 2 in ref 40) because these density data are free from effects observed in smaller capillaries and represent bulk water data. TMD of D_2O is higher by 7 deg than that of H_2O, but this difference is roughly compensated by a lowering of TMD in "dilute" 2 M D_2O solution. The similar temperature dependence of the two sets of data below 275 K is remarkable, and it suggests a common origin in the structural changes of supercooled water.

The anomalous increase of water's thermodynamic quantities on supercooling has stimulated an enormous amount of experimental, theoretical, and computational work in an attempt to understand its microscopic origin (see the remarkable review by Debenedetti[3]). Three different thermodynamic scenarios have been proposed for the thermodynamic anomalies of supercooled water which are the existence of a continuous, retracing spinodal curve bounding the superheated, stretched, and supercooled states of liquid water,[57] the existence of a metastable, low-temperature critical point,[58] and the progressive increase of tetrahedrally connected hydrogen-bonded water molecules on supercooling.[59,60] The first two scenarios assume some form of critical behavior. The third one is a singularity-free interpretation, and it shows that "the increase in compressibility upon lowering the temperature of a liquid that expands on cooling, like water, is not contingent on any singular behavior, but rather is a thermodynamic necessity".[60] Considering the variety of scenarios for understanding the anomalous

properties of supercooled water, it is premature to speculate on the anomalous increase in contact-ion pairing in more detail.

Johari[61] recently argued that, for the water-in-oil emulsion measurements, a substantial fraction of the anomalously high C_p and volume of supercooled water is due to intergranular premelting effects. This interesting argument suggests further experimental studies of emulsified supercooled water, but it does not apply to the molar volume measurements of supercooled water in capillaries with 0.3 mm inner diameter reported by Hare and Sorensen.[40]

Estimation of Average Fictive Temperature on Hyperquenching. The average fictive temperature, T_f,[13,14] where water becomes structurally immobilized on hyperquenching, is of considerable theoretical and practical importance first for estimates of the thermodynamic path water takes on hyperquenching into the glassy state[15,16] and second because below water's T_f structural and conformational changes of a solute are expected to cease.[17−20,62,63] For example, for pure 2-chlorobutane freezing in of its rapidly interconverting conformers occurs on slow cooling at ≈97 K, but for 2-chlorobutane dissolved in Nujol exchange between its conformers stops already at ≈205 K, which is close to the T_f of the solvent.[62,63] Fishman et al.[63] have developed an IR spectroscopic method for obtaining a solvent's T_f value by determining the temperature where conformer exchange of a solute stops. Here we use the temperature dependence of contact-ion pairing in 2 M $Ca(NO_3)_2$ D_2O solution as a probe for our estimation of D_2O water's T_f value on hyperquenching into the glassy state. This estimation can give only an average T_f first, because in a glass cooled at a given rate, a distribution of relaxation times and T_f values is observed[14,64] which is the limitation of the fictive temperature concept.[14] And second, we expect in addition that the liquid droplets experience a distribution of cooling rates, depending among others on the contact with the cold substrate when it consists of a layer of already quenched, flattened droplets (see Figure 1b in ref 65).

At ambient temperature, water exchange in the first hydration sphere of the Ca^{2+} ion is a highly dynamic process, close to diffusion controlled,[66,67] and similar dynamics is reported for anions. For Ca^{2+}, after removal of a water molecule, subsequent binding is also close to diffusion controlled which makes Ca^{2+} one of the most efficient biological triggers (Table 4.3 in ref 66). We thus expect that formation of a contact-ion pair, with Ca^{2+} as cation, from a solvent-shared and/or solvent-separated ion pair is also a highly dynamic process and that this contact-ion pair formation is structurally arrested only once water has been immobilized. This is a prerequisite for using changes in contact-ion pairing of a solute as indicator for the solvent's T_f.

In Figure 8 the logarithm of the I_B/I_F area ratios in 2 M $Ca(NO_3)_2$ D_2O solution is plotted against reciprocal temperature. The ln of the I_B/I_F value for the 2 M hyperquenched glassy solution recorded at 80 K is drawn as a horizontal line. The two broken lines indicate an upper and lower temperature limit for extrapolation of the experimental data points to the I_B/I_F value of the 2 M glassy solution. These give an approximate temperature range of immobilization, or average T_f value, of 200−230 K. As expected, T_f obtained by this extrapolation is much higher than the T_g value of 137 K calorimetrically determined by heating hyperquenched glassy D_2O water at a rate of 30 K min^{-1},[11,12] and similar T_g values were obtained on heating "dilute" glassy electrolyte H_2O solutions.[68] A T_g value of between 200 and 230 K would be observable on reheating only when the sample is heated with the same rate as it had been quenched before. An analysis of the dependence of T_g on cooling and heating rate is given in ref 69. For H_2O solutions, the temperature range of immobilization is expected to be only slightly lower.[12]

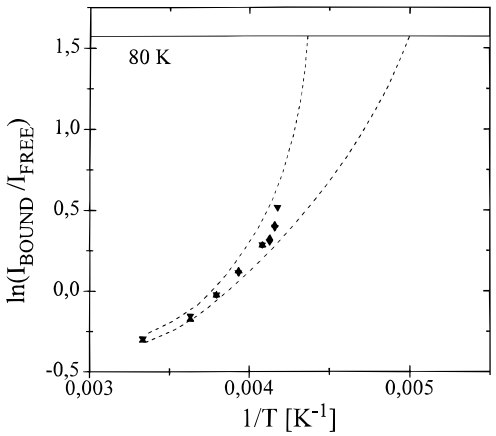

Figure 8. Plot of $\ln(I_{BOUND}/I_{FREE})$ area ratios versus reciprocal temperature for the data of the emulsified solution from Figure 3. The plot further contains as horizontal line the $\ln(I_{BOUND}/I_{FREE})$ value for 2 M solution hyperquenched into the glassy state and recorded at 80 K. The two broken lines are our extrapolated upper and lower temperature estimate for the temperature range where contact-ion pairing is structurally arrested on hyperquenching into the glassy state.

The extrapolation presupposes thermodynamic continuity of states between normal and supercooled water (or dilute aqueous solution) and the glassy water (or glassy dilute solution) obtained on hyperquenching. Thermodynamic discontinuity between liquid and glassy water had been proposed by Speedy from an analysis of water's enthalpy at 236 and 150 K,[15] but recent experimental studies are consistent with a continuity of states.[70−73]

Our estimation of the temperature range where structural arrest occurs is of theoretical importance for estimates of the thermodynamic path water takes on hyperquenching into the glassy state.[15,16] Johari et al.[16] have analyzed the effects of two different cooling rates: one where the rate was such that configurational freezing of the water's structure may have occurred at 200 K and a lower one where it may have occurred at 180 K. The frozen-in configurational enthalpy and entropy depend on both the temperature of immobilization and the thermodynamic path liquid water takes on hyperquenching into the glassy state. According to our T_f estimation a third, higher, temperature, e.g., 220 K, should also be considered in such an analysis.

Comparison of T_f Estimate with Calculations of the "Kinetic Glass Transition". Our estimation of the temperature range where the 2 M $Ca(NO_3)_2$ D_2O solution is immobilized on hyperquenching into the glassy state, is next compared with recent molecular dynamics (MD) calculations of deeply supercooled SPC/E water and its kinetic glass transition.[32−35] These calculations were done in order to rationalize the experimentally observed non-Arrhenius increase of the transport coefficients on supercooling without invoking the presence of hidden thermodynamics anomalies at ambient pressure.[1,2] Evidence in favor of a mode coupling theory (MCT) description of the slow collective dynamics in deeply supercooled simulated SPC/E and for a two step relaxation process have been presented, with the cage formation being controlled by the formation of an open network of hydrogen bonds. In these simulations SPC/E water undergoes a kinetic glass transition (or critical temperature of MCT) about 50 degrees below TMD for SPC/E. This is remarkably close to the so-called Speedy-Angell temperature of ≈228 ± 3 K for thermodynamic and transport properties of supercooled water.[1,57] The conclusion was that the experimen-

tally observed divergence of transport properties in supercooled water can be described by MCT and does not need to rely on a thermodynamic instability.[33−35]

For our comparison we have to take into account first, that D_2O was used as solvent instead of H_2O, and second, the effect of the electrolyte. For supercooled D_2O the Speedy-Angell temperature is at ≈233 K.[1,2] The increase of ≈5 degrees by using D_2O instead of H_2O is for dilute solution roughly compensated by the effect of the solute.[75] Therefore, our range of T_f values obtained by extrapolation can be compared with the Angell temperature of 228 K for H_2O water and the kinetic glass transition of SPC/E water.[32−35] This comparison shows that both, the Speedy-Angell temperature and the kinetic glass transition temperature of SPC/E water correspond to our extrapolated estimate of the upper temperature limit for immobilization of ≈230 K (see Figure 8). This is consistent with Sciortino et al.'s conclusion that the "divergence of transport coefficients does not need to rely on a thermodynamic instability".[34,35]

Contact-Ion Pairing in "Concentrated" versus "Dilute" Solution. For the "concentrated" 5 M solution, both evaluation of the ν_4 band region and the combination band region gives a decrease in relative area of the component band assigned to contact-ion pairs on cooling (Figures 5 and 6). This is consistent with Spohn and Brill's Raman spectroscopic study of 5.48 m $Ca(NO_3)_2$ solution where the relative area of bound nitrate increased in a linear way from ≈15% at 296 K to ≈90% at 723 K (read from Figure 13 in ref 31). A direct comparison of their values with ours is not possible first, because we had to use a higher $Ca(NO_3)_2$ concentration (5.00 M is 6.5 m) in order to avoid formation of ice on slow cooling, and second, for the ν_4 band region the molar infrared intensity of bound nitrate is much larger than that of "free" nitrate whereas the molar Raman intensities are equal.[23,29]

The calorimetric T_g value of 5 M $Ca(NO_3)_2$ H_2O solution obtained on heating at 10 K min^{-1} is at 184 K (read from Fig. 3 in ref. 75), and the T_g value of the D_2O solution is expected to be only a few degrees higher. Therefore, contact-ion pairing is structurally arrested on slow cooling the 5 M solution at ≈190 K, whereas on hyperquenching structural arrest occurs according to our estimation in Figure 8 between 230 and 200 K. Figures 5 and 6 show that at 80 K I_B/I_F band area ratios are the same within experimental error. This indicates that only minor changes in contact-ion pairing can have occurred in this small temperature range.

Cryofixation of Biomolecules. Our T_f estimation is of practical importance for so-called cryofixation because it is the low-temperature limit where structural changes can occur in a solute on hyperquenching its aqueous solution into the glassy state. The goal of cryofixation is to immobilize, or "freeze-in", the native state of dynamic structures and the momentary distribution of all components in a system (for reviews see ref 17 and 18). This is impossible for highly mobile small molecules and ions even by hyperquenching, as shown in this and our earlier studies by increasing contact-ion pairing with decreasing temperature. Whether or not the conformer population of a biomolecule at ambient temperature can be immobilized, or frozen-in, depends on the relative rates of cooling and of conformer interconversion and on their temperature dependencies. Apparently the highest cooling rates are the best ones for immobilizing the structure and the conformer population of a biomolecule close to ambient temperature for subsequent further studies at cryogenic temperatures. These techniques were developed for vitrifying water and dilute aqueous solutions[4,5] at estimated[17] and calculated[76] rates of ≈10^6 to ≈10^7 K s^{-1}, and they were adapted for use in cryoelectron microscopy.[5,18] We have recently reported two FT-IR spectroscopic studies of cryofixation of aqueous solutions of carbonylhemoglobin (HbCO) and metmyoglobin azide conformer populations which nicely demonstrate the wide range of temperatures possible for structural arrest of a solute:[19,20] at ambient temperature for HbCO the rate of its CO conformer interconversion is $>10^4$ s^{-1} (ref 77) whereas for metmyoglobin azide the rate of its high spin/low spin interconversion is $>2 \times 10^5$ s^{-1} (ref 78). These FT-IR spectroscopic studies showed that HbCO's CO conformer interconversion is frozen-in by hyperquenching close to ambient temperature,[20] whereas for metmyoglobin azide structural arrest of the even more dynamic high spin/low spin equilibrium must have occurred in the temperature range of the T_f estimate.[19] In the latter case when structural changes occur in a biomolecule despite cooling at a very high rate, conformational/structural changes can be induced by increase in contact-ion pairing because contact-ion pairs (or salt bridges) can contribute significantly to the stability of a protein.[79,80]

Acknowledgment. We are grateful for financial support by the Forschungsförderungsfonds of Austria (FWF project P12319-PHY).

Supporting Information Available: Five tables containing the curve-fitting parameters to Figures 2, 5, and 6 (5 pages). Ordering information is given on any current masthead.

References and Notes

(1) Angell, C. A. In *Water, a comprehensive treatise*; Franks, F., Ed.; Plenum Press: New York, 1982; Vol. 7, Chapter 1.
(2) Angell, C. A. *Annu. Rev. Phys. Chem.* **1983**, *34*, 593.
(3) Reviewed recently by: Debenedetti, P. G. *Metastable Liquids*; Princeton University Press: Princeton, 1996.
(4) Brüggeller, P.; Mayer, E. *Nature* **1980**, *288*, 569. Mayer, E.; Brüggeller, P. *Nature* **1982**, *298*, 715. Mayer, E. *J. Appl. Phys.* **1985**, *58*, 663; *J. Microsc.* **1986**, *140*, 3.
(5) Dubochet, J.; McDowell, A. W. *J. Microsc.* **1981**, *124*, RP3.
(6) Hallbrucker, A.; Mayer, E.; O'Mard, L. P.; Dore, J. C.; Chieux, P. *Phys. Lett. A* **1991**, *159*, 406.
(7) Bellissent-Funel, M. C.; Bosio, L.; Hallbrucker, A.; Mayer, E.; Sridi-Dorbez, R. *J. Chem. Phys.* **1992**, *97*, 1282.
(8) Dore, J. C. In *Water Science Reviews*; Franks, F., Ed.; Cambridge University Press: Cambridge, 1985; Vol. 1; Chapter 1; *J. Mol. Struct.* **1990**, *237*, 221.
(9) Chen, S. H.; Teixeira, J. *Adv. Chem. Phys.* **1986**, *64*, 1.
(10) Bellissent-Funel, M.-C.; Teixeira, J.; Bosio, L.; Dore, J. C. *J. Phys. (Paris)* **1989**, *C1*, 7123. Bellissent-Funel, M.-C.; Bosio, L. *J. Chem. Phys.* **1995**, *102*, 3727.
(11) Johari, G. P.; Hallbrucker, A.; Mayer, E. *Nature* **1987**, *330*, 552.
(12) Hallbrucker, A.; Mayer, E.; Johari, G. P. *Philos. Mag.* **1989**, *60B*, 179. Johari, G. P.; Hallbrucker, A.; Mayer, E. *J. Chem. Phys.* **1990**, *92*, 6742.
(13) Tool, A. Q. *J. Am. Ceram. Soc.* **1946**, *29*, 240.
(14) Ritland, H. N. *J. Am. Ceram. Soc.* **1956**, *39*, 403. Rekhson, S. M. *J. Non-Cryst. Solids* **1986**, *84*, 68.
(15) Speedy, R. J. *J. Phys. Chem.* **1992**, *96*, 2322.
(16) Johari, G. P.; Fleissner, G.; Hallbrucker, A.; Mayer, E. *J. Phys. Chem.* **1994**, *98*, 4719.
(17) Plattner, H.; Bachmann, L. *Int. Rev. Cytol*. **1982**, *79*, 237. Robards, A. W.; Sleytr, U. B. *Low-Temperature Methods in Biological Electron Microscopy*; Elsevier: New York, 1985; Chapter 2. Bachmann, L.; Mayer, E. In *Cryotechniques in Biological Electron Microscopy*; Steinbrecht, R. A., Zierold, K., Eds.; Springer-Verlag: Berlin, 1987; pp 1−34. Knoll, G.; Verkleij, A. J.; Plattner, H. Ibid., pp 258−271. Sitte, H.; Edelmann, L.; Neumann, K. Ibid., pp 87−113. Kellenberger, E. Ibid., pp 35−63.
(18) Dubochet, J.; Adrian, M.; Chang, J.-J.; Homo, J. C.; Lepault, J.; McDowall, A. W.; Schultz, P. *Q. Rev. Biophys.* **1988,** *21*, 129−228.
(19) Mayer, E.; Astl, G. *Ultramicroscopy* **1992**, *45*, 185.
(20) Mayer, E. *J. Am. Chem. Soc.* **1994**, *116*, 10571.
(21) Mayer, E. *J. Phys. Chem.* **1985**, *90*, 4455.
(22) Hage, W.; Hallbrucker, A.; Mayer, E. *J. Phys. Chem.* **1992**, *96*, 6488.

(23) Fleissner, G.; Hallbrucker, A.; Mayer, E. *J. Phys. Chem.* **1993**, *97*, 4806.
(24) Fleissner, G.; Hallbrucker, A.; Mayer, E. *Chem. Phys. Lett.* **1994**, *218*, 93.
(25) Fleissner, G.; Hallbrucker, A.; Mayer, E. *J. Phys. Chem.* **1995**, *99*, 8401.
(26) Fleissner, G.; Hallbrucker, A.; Mayer, E. *J. Chem. Soc., Faraday Trans.* **1996**, *92*, 23.
(27) Petrucci, S. In *Ionic Interactions*; Petrucci, S., Ed.; Academic Press: New York, London, 1971; Vol. I, Chapter 3.
(28) Franck, U. E. *Pure Appl. Chem.* **1981**, *53*, 1401.
(29) For review of older literature see: Irish, D. E.; Brooker, M. H. In *Advances in Infrared and Raman Spectroscopy*; Clark, R. J. H., Hester, R. E., Eds.; Heyden: London, 1976; Vol. 2, Chapter 6.
(30) Irish, D. E.; Jarv, T. *Appl. Spectrosc.* **1983**, *37*, 50.
(31) Spohn, P. D.; Brill, T. B. *J. Phys. Chem.* **1989**, *93*, 6224.
(32) Baez, L. A.; Clancy, P. *J. Chem. Phys.* **1994**, *101*, 9837.
(33) Gallo, P.; Sciortino, F.; Tartaglia, P.; Chen, S.-H. *Phys. Rev. Lett.* **1996**, *76*, 2730.
(34) Sciortino, F.; Gallo, P.; Tartaglia, P.; Chen, S.-H. *Phys. Rev. E* **1996**, *54*, 6331.
(35) Sciortino, F.; Fabbian, L.; Chen, S.-H.; Tartaglia, P. *Phys. Rev. E*, submitted.
(36) Mayer, E. *Chem. Phys. Lett.* **1987**, *139*, 370.
(37) Broto, F.; Clause, D. *J. Phys. (Paris)* **1976**, *C9*, 4251.
(38) Fleissner, G.; Hage, W.; Hallbrucker, A.; Mayer, E. *Appl. Spectrosc.* **1996**, *50*, 1235.
(39) Hare, D. E.; Sorensen, C. M. *J. Chem. Phys.* **1990**, *93*, 25; **1990**, *93*, 6954; **1992**, *96*, 13.
(40) Hare, D. E.; Sorensen, C. M. *J. Chem. Phys.* **1987**, *87*, 4840.
(41) Hester, R. E.; Plane, R. A. *J. Chem. Phys.* **1964**, *40*, 411.
(42) Irish, D. E.; Walrafen, G. E. *J. Chem. Phys.* **1967**, *46*, 378.
(43) Gill, J. B. *Pure Appl. Chem.* **1981**, *53*, 1365.
(44) Fleissner, G. Ph.D. Thesis, University of Innsbruck, Innsbruck/Austria, 1995.
(45) Firman, P.; Xu, M.; Eyring, E. M.; Petrucci, S. *J. Phys. Chem.* **1992**, *96*, 8631.
(46) Irish, D. E.; Ozeki, T. In *Analytical Raman Spectroscopy*; Grasselli, J. G., Bulkin, B. J., Eds.; Chemical Analysis Series 1991; Vol. 114, pp 59−106.
(47) Chang, T. G.; Irish, D. E. *J. Phys. Chem.* **1973**, *77*, 52. Chang, T. G.; Irish, D. E. *J. Solution Chem.* **1974**, *3*, 161; **1974**, *3* 175.
(48) Angell, C. A.; Oguni, M.; Sichina, W. J. *J. Phys. Chem.* **1982**, *86*, 998.
(49) Lever, A. B. P.; Mantovani, E.; Ramaswamy, B. S. *Can. J. Chem.* **1971**, *49*, 1957.
(50) Hallbrucker, A.; Mayer, E. *J. Phys. Chem.* **1988**, *92*, 2007.
(51) Sorensen, C. M. *J. Chem. Phys.* **1983**, *79*, 1455.
(52) Angell, C. A.; Tucker, J. C. *J. Phys. Chem.* **1980**, *84*, 268.
(53) Fuoss, R. M. *J. Am. Chem. Soc.* **1958**, *80*, 5059.
(54) Quist, A. S.; Marshall, W. L. *J. Phys. Chem.* **1965**, *69*, 3165.
(55) Bertolini, D.; Cassetari, M.; Salvetti, G. *J. Chem. Phys.* **1982**, *76*, 3285.
(56) Chingakule, D. D. K.; Gans, P.; Gill, J. B.; Longdon, P. J. *Chem. Monthly* **1992**, *123*, 521.
(57) Speedy, R. J.; Angell, C. A. *J. Chem. Phys.* **1976**, *65*, 851. Speedy, R. J. *J. Chem. Phys.* **1982**, *86*, 982.
(58) Poole, P. H.; Sciortino, F.; Essmann, U.; Stanley, H. E. *Nature* **1992**, *360*, 324. Poole, P. H.; Sciortino, F.; Grande, T.; Stanley, H. E.; Angell, C. A. *Phys. Rev. Lett.* **1994**, *73*, 1632.
(59) Stanley, H. E.; Teixeira, J. *J. Chem. Phys.* **1980**, *73*, 3404.
(60) Sastry, S.; Debenedetti, P. G.; Sciortino, F.; Stanley, H. E. *Phys. Rev. E* **1996**, *53*, 6144.
(61) Johari, G. P. *J. Chem. Phys.* **1997**, *107*, 10154.
(62) Fishman, A. I.; Stolov, A. A.; Remizov, A. B. *Spectrochim. Acta* **1993**, *49A*, 1435.
(63) Fishman, A. I.; Guseva, S. Y.; Remizov, A. B.; Stolov, A. A.; Zgadzai, O. E. *Spectrochim. Acta* **1986**, *42A*, 1247.
(64) Johari, G. P.; Hallbrucker, A.; Mayer, E. *J. Phys. Chem.* **1989**, *93*, 2648.
(65) Mayer, E. In *Hydrogen Bond Networks*; Bellissent-Funel, M.-C., Dore, J. C., Eds.; Kluwer Academic Publ.: Dordrecht, The Netherlands, 1994; p 355.
(66) daSilva, J. J. R.; Williams, R. J. P. *The Biological Chemistry of the Elements*; Oxford, 1991; Chapter 4.
(67) Burgess, J. *Ions in Solution*; E. Horwood: New York, 1988; p 112.
(68) Hofer, K.; Hallbrucker, A.; Mayer, E.; Johari, G. P. *J. Phys. Chem.* **1989**, *93*, 4674. Hofer, K.; Astl, G.; Mayer, E.; Johari, G. P. *J. Phys. Chem.* **1991**, *95*, 10777.
(69) Sasaba, H.; Moynihan, C. T. *J. Polym. Sci., Polym. Phys. Ed.* **1978**, *16*, 1447 and references therein. Vollmayr, K.; Kob, W.; Binder, K. *J. Chem. Phys.* **1996**, *105*, 4714.
(70) Speedy, R. J.; Debenedetti, P. G.; Huang, C.; Smith, R. C.; Kay, B. D. In *Physical Chemistry of Aqueous Systems: Meeting the Needs of Industry*; Proceedings of the 12th International Conference on the Properties of Water and Steam; White Jr., H. J., Sengers, J. V., Neumann, D. B., Bellows, J. C., Eds.; Begell House: New York, 1995; p 347.
(71) Speedy, R. J.; Debenedetti, P. G.; Smith, R. S.; Huang, C.; Kay B. D. *J. Chem. Phys.* **1996**, *105*, 240.
(72) Smith, R. S.; Huang, C.; Kay, B. D. *J. Phys. Chem. B* **1997**, *101*, 6123.
(73) Walrafen, G. E.; Chu, Y. C. *J. Phys. Chem.* **1995**, *99*, 11225.
(74) Oguni, M.; Angell, C. A. *J. Chem. Phys.* **1980**, *73*, 1948; **1983**, *78*, 7334.
(75) Angell, C. A.; Sare, E. J. *J. Chem. Phys.* **1970**, *52*, 1058.
(76) Bald, W. B. *J. Microsc.* **1986**, *143*, 89.
(77) Potter, W. T.; Hazzard, J. H.; Choc, M. G.; Tucker, M. P.; Caughey, W. S. *Biochemistry* **1990**, *29*, 6283.
(78) Beattie, J. K.; West, R. J. *J. Am. Chem. Soc.* **1974**, *96*, 1933.
(79) Perutz, M. F. *Science* **1978**, *201*, 1187.
(80) Jaenicke, R. *Philos. Trans. R. Soc. London, Ser. B* **1990**, *326*, 535.